AIAA JOURNAL
Vol. 39, No. 4, April 2001

Controlling Vibrational Chaos of a Curved Structure

Lucio Maestrello*
NASA Langley Research Center, Hampton, Virginia 23681-2199

Nonlinear response of a flexible curved panel exhibiting bifurcation to fully developed chaos is demonstrated along with the sensitivity to small perturbations from the initial forcing. The response is determined from the measured time series at two fixed points. The panel is forced by an external nonharmonic multifrequency and monofrequency sound field. Using a low-power time-continuous control, carefully tuned to each initial forcing condition, produces large long-term effects on the dynamics toward taming chaos. Without knowledge of the initial forcing, control may be achieved by destructive interference. In this case, the control power is proportional to the loading power. Calculation of the correlation dimension and the estimation of positive Lyapunov exponents, in practice, are the proof of chaotic response.

I. Introduction

DYNAMIC instability and chaos are now established to be common features of many nonlinear processes in engineering, physics, climatology, medicine, astronomy, biology, neuronal science, and ecology. Chaos manifests beneficial as well as destructive effects. Detecting nonlinearity is considerably easier than identifying chaotic dynamics. The most common and useful tool for the characterization of chaos is the estimation of the correlation dimension and the Lyapunov exponent from an experimental time series. Nonlinear analyses of time series, and especially methods based on chaos theory, have probably contributed toward a better understanding of many observed physical phenomena. Structural dynamics and acoustics responses have demonstrated the existence of strong nonlinear behaviors when forced by high acoustic loading; as a result, appropriate dynamic control techniques have been implemented to stabilize the system. The control algorithm proposed by Ott, Grebogi, and Yorke (OGY)[1] has been used in many applications to stabilize an unstable periodic orbit through the application of small, carefully selected perturbations aimed at establishing control over chaotic response.[2–7] The control method used is different from the OGY method. It is a simple method requiring the knowledge of the initial unstable disturbances in terms of frequency, amplitude, and phase to cancel the growth after several bifurcations for periodicity and chaotic responses using a small external forcing to reduce the response. No intelligent feedback exists between what the system is doing and the resulting actuation; the control system is a feedforward, open-loop system. Control of chaos using controllers that are very simple relative to the system being controlled is discussed by Braiman and Goldhirsch[8] and by Corron et al.[9] The present experiment is designed to control the chaotic response via initial forcing by changing the system dynamics of a curved panel structure loaded by high-intensity sound.

Instability and chaos, two of the main concepts associated with nonlinear vibration, have revolutionized our understanding about the response of a dynamic system. Because there is no universal set of eigenfunctions for a nonlinear system, most data analyses are performed in the time domain. Because of the complicated dynamics of the response, prediction is impossible over extended time; however, the experiments are done to gain insight into the limitations set by nonlineality.[10–14] In our experiments, the linear system fails to describe structural response induced by high-intensity sound. Stochastic measurements are not useful because they concentrate on average quantities such as correlation coefficients and autocorrelation functions, and they are not able to distinguish between the data from a linear system and those from a nonlinear system, whereas short-term measurements reveal the time limit of a reliable prediction. One cannot repeat the experiment exactly because of the changes in the initial forcing because this is one of the most peculiar features of a nonlinear chaotic response.[15] In a previous experiment, a panel forced by constant or accelerated flow and sound exhibits different dynamics for each experimental run; this indicates the dependency on the unpredictable initial forcing.[10,16] Furthermore, tension and curvature of the structure depend on the loading, and they constitute a coupling with the response; one manifestation is spontaneous surface deformation. Some related problems are elastic structures forced by jet noise, turbulent boundary layer at constant and accelerated speed, and flutter behaviors such as wings and panels with various nonlinearities.[17–25] Military aircraft structure is forced by an external jet of a level of 160 dB, which is 20 dB above the level of the present experiment. An example related to medical science is that the heart under normal conditions has a periodic rhythm; however, as one nears a heart attack, it becomes chaotic,[26] and in neurophysiology, nonlinear science is used to clarify the principles of the functioning of the brain. We explore how chaotic response of a flexible curved panel forced by external single and nonharmonic multifrequency sound can be controlled by using active control with the knowledge of the initial forcing. Without the knowledge of the initial forcing, control is achievable by the equilibrium of forces and by damping.[27] Traditional control methods have avoided chaotic responses, which comprise a large and rich part of the physical system. The initial forcing is unknown in a time series of unknown origin; therefore, a technique is introduced to determine the initial forcing by using the time series of the experimental data.[15,28,29] From the data, we want to determine whether the system response is chaotic by using techniques drawn from classical dynamics. One can argue that the time series has been generated by a random field; however, the definition of chaos includes three elements: 1) determinism, 2) aperiodicity, and 3) sensitive dependence on initial conditions.[30,31]

This paper begins by describing the instrumentation followed by the description of a technique used to determine the initial forcing and the description of the panel response and the method used for active control. The paper is organized as follows. Section II discusses instrumentation. Analysis of the data is reported in Sec. III. Results are given in Sec. IV, with Sec. IV.A describing the wall pressure, Sec. IV.B describing the panel response, Sec. IV.B.1 describing a search for initial forcing, Sec. IV.B.2 describing panel response and active control from multifrequency sound, and section IV.C describing panel response and active control from monofrequency sound. Section V discusses the correlation dimensions and Lyapunov exponents.

II. Instrumentation

The experiment is set up to study the nonlinear response of panels excited by plane acoustic waves at normal and oblique incidences.

Received 19 November 1999; presented as Paper 2000-2016 at the AIAA/CEAS 6th Aeroacoustics Conference, Lahaina, HI, 12–14 June 2000; revision received 25 August 2000; accepted for publication 1 September 2000.

*Scientist, Aerodynamics, Aerothermodynamics and Acoustics Competency.

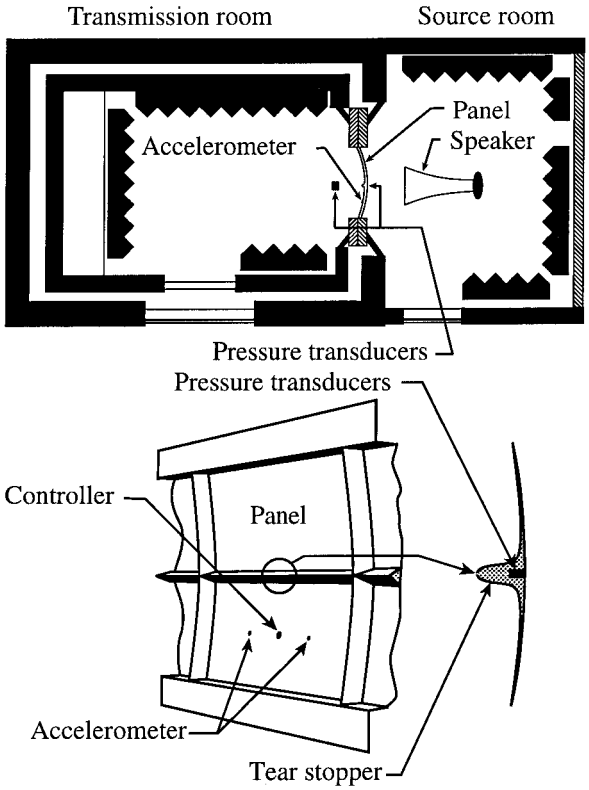

Fig. 1 Experimental setup.

The panels are curved airplane fuselage types made of 6061-T6 aluminum machined from a plate into two panels separated by a longitudinal tear stopper. The tear stopper has a 0.5-cm radius of curvature (arc length) to minimize the amplitude of the reflected and transmitted waves. The structure is 0.609 m wide, 1.019 m long, and 0.109 cm thick, with a radius of curvature of 2.529 m. The two panels are the same size, and the structure is mounted in a rigid partition dividing two anechoic rooms, the source and the transmission rooms (see Fig. 1). The acoustic sources are created by four 120-W phase-amplitude matched speakers mounted in a horn diffuser and are capable of generating approximately 138 dB of acoustic power. The wall pressure fluctuations are measured with miniature pressure transducers mounted flush within the tear stopper between panels. The vibration response is measured with two miniature accelerometers located at one-quarter length and three-quarter length of the panel on the centerline. The transmitted pressure is measured with a pressure transducer. The active controller is a feedforward, open-loop system. The control actuator is mounted at the center of the lower panel and is freely suspended. Two accelerometer signals provide the output signal from the panel motion. Another accelerometer is placed at the shaker–panel interface. All measurements are made from direct-current response.

III. Experimental Technique and Data Analysis

The nonlinear time series for short-time signal processing is the basic tool used to analyze the experimental data. They are applied to input and transmitted pressure and panel response. A limited number of dynamic variables and positions can be measured on the panel. The key element in resolving the problem is that the full system phase space has one-to-one correspondence with the measurements

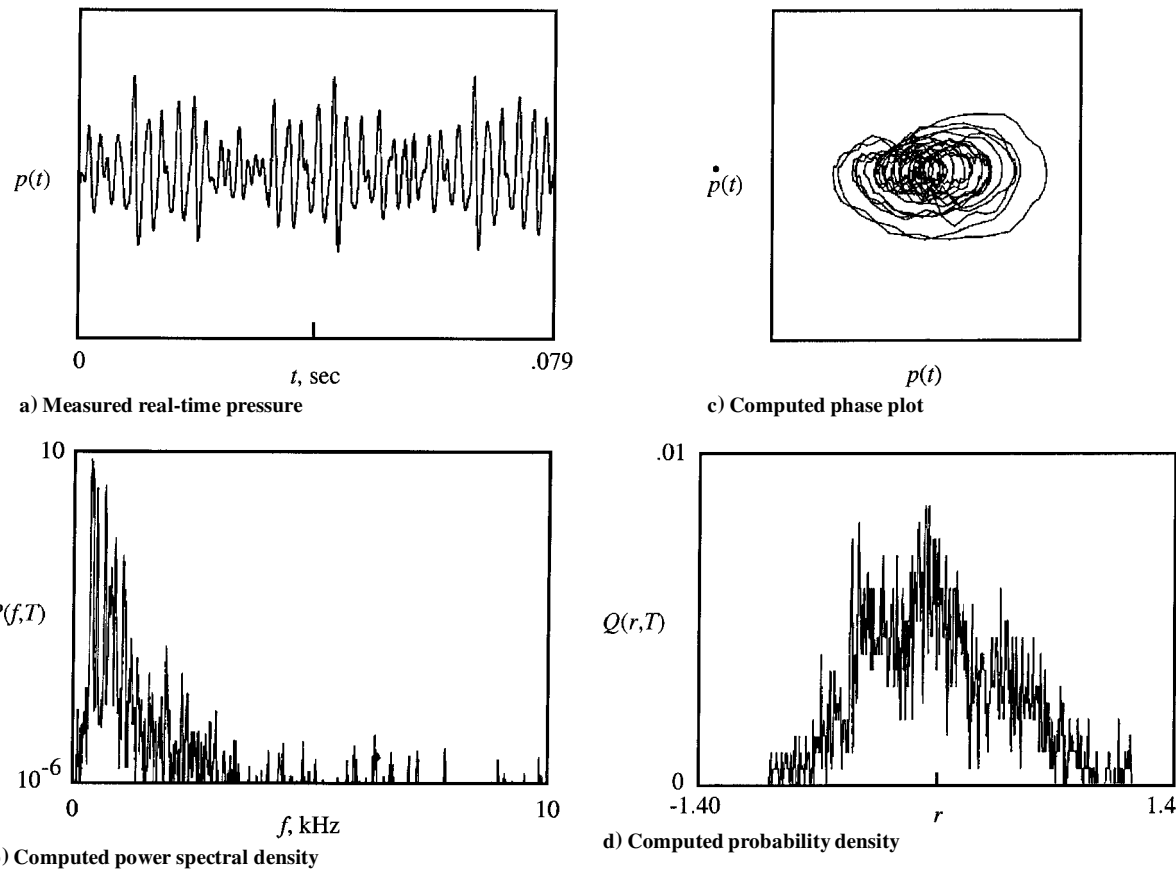

Fig. 2 Normalized wall pressure fluctuation.

of a limited number of point and variables. Local properties of the dynamics for readers unfamiliar with them are as follows.

1) Energy variance is a technique used to locate unstable orbits and consists of time series, spectrum, phase portrait, probability, and Poincaré map.

2) Initial forcing determine whether the trajectory of the attractor diverges exponentially.

3) Correlation dimension is the number of degrees of freedom.

4) Lyapunov exponent governs the exponential divergence in the neighboring trajectories in a nonlinear system; thus, the sign of the Lyapunov exponent determines the behavior.

The time history of the wall pressure fluctuation and panel acceleration is measured; the power spectral density, the phase portrait, and the probability distribution are computed from it. For a nonstationary signal $q(t, x)$, such as the pressure fluctuation $p(t, x)$ and the panel acceleration $g(t, x)$, the instantaneous power spectrum at instant T is defined by

$$P(f, T) = \left| \frac{1}{2\pi} \int_{T-I/2}^{T+I/2} \exp(i2\pi f t) q(t, x)\, \mathrm{d}t \right|^2$$

where T is chosen so that the experimental run contains the interval $T - I/2, T + I/2$ for a sufficiently large I. The probability density of $\hat{q}(T, x)$ is denoted by $Q(r, T)$, where

$$\hat{q}(T, x) = \frac{1}{I} \int_{T-I/2}^{T+I/2} q(t, x)\, \mathrm{d}t$$

$$Q(r, T) = \frac{\mathrm{d}}{\mathrm{d}r} \text{prob}\, \hat{q}(T, x) \le r]$$

In chaotic dynamics, searching for a low-dimensional characterization of the system is of great interest. Let $q(t, x)$ be a measured temporal signal or time series at position x, which is embedded in a d-dimensional phase space by a time delay τ. Let $z_1(t) = q(t, x)$, $z_2(t) = z_1(t + \tau)$, and $z_d(t) = z_1(t + d\tau)$. The set $Z(t) = z_1(t), \ldots, z_d(t)]$ for $t \ge 0$ is regarded as a trajectory in the d-dimensional phase space. The distance between two points $Z(t_i)$ and $Z(t_j)$ is given by d_{ij}, and for a small $\varepsilon > 0$, let $N_d(n, \varepsilon)$ be the number of pairs of points with distance $d_{ij} < \varepsilon$. Then the correlation sum $C_d(\varepsilon)$ and the correlation dimension $D(d)$, for given d, are defined by Grassberger and Procaccia[32] as

$$C_d(\varepsilon) = \lim_{n \to \infty} \frac{2N_d(n, \varepsilon)}{n(n-1)}$$

$$D_d = \lim_{\varepsilon \to 0} \frac{\log C_d(\varepsilon)}{\log \varepsilon}$$

For computation, the parameters τ and d must be chosen properly, and the correlation dimension D_d is estimated by

$$D_d \approx \frac{\log C_d(n, \varepsilon)}{\log \varepsilon}$$

for a sufficiently small ε and large n. The estimated dimension D is taken as the asymptotic value of D_d as the embedding dimension d increases.

Given the estimated dimension D and using the method advocated by Grassberger and Procaccia,[32] the Lyapunov exponent, which is one of the most important characteristics in the dynamics system, can be approximately computed. Several methods exist for computing the Lyapunov exponents.[15,28,29,32–35] The Eckmann–Ruelle method[34] is used herein. Consider $Z(t)$, $t \ge t_0$, as the trajectory of a dynamic system in the phase space of dimension $d = D$. For $i = 1, 2 \ldots$, let the local tangent line approximations for the trajectory at time t be denoted by T_i, known as the tangent (linear) maps. The dynamic system is reconstructed by a least-squares fit to these linear approximations. Technically decomposing T_i into an orthogonal matrix Q_i and an upper triangular matrix U_1 by $T_1 = Q_1 R_1$ and U_i by $T_i Q_{i-1} = Q_i R_i$, for $i \ge 2$, the Lyapunov exponents can be computed as follows:

$$\lambda_i = \lim 1/(k-1)] \log|(R_{k-1}, \ldots, R_2 R_1)_{ii}|$$

for $i = 1, 2, \ldots, D$. For details, see the Eckmann–Ruelle algorithm given by Maestrello[16] and Conte and Dubois.[33]

IV. Results

Time series for short-time signal processing is applied to identify the input wall pressure and panel response to describe the complex surface vibration. The time series of chaotic signals has broadband components, and we select the loading frequencies on the basis of the maximum acoustic power delivered by the acoustic drivers and on the level of the panel response.

A. Wall Pressure

The surface pressure fluctuations with 138-dB input acoustic power were measured on the rigid surface of the tear stopper between panels because the pressure transducer cannot be mounted on the vibrating panel without altering its response (Fig. 1). The loading

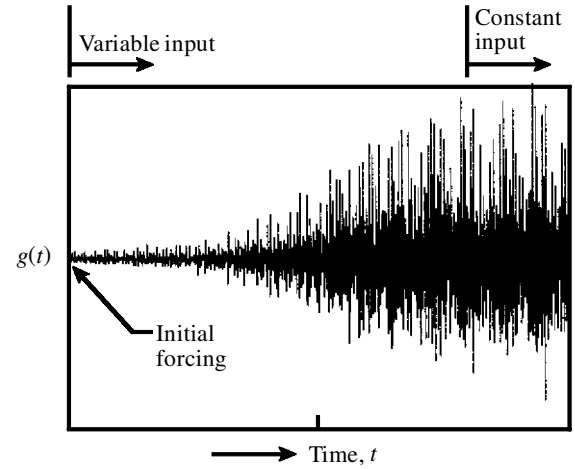

Fig. 3 Temporal evolution of the panel acceleration response; loading induced by the frequencies $f_1 = 387, f_2 = 425, f_3 = 512$, and $f_4 = 687$ Hz.

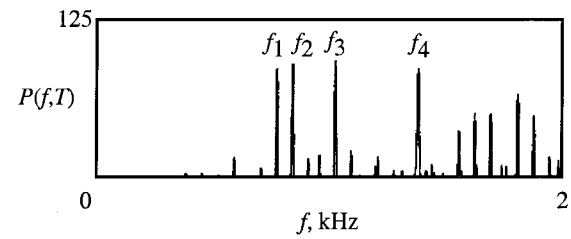

a) Input pressure

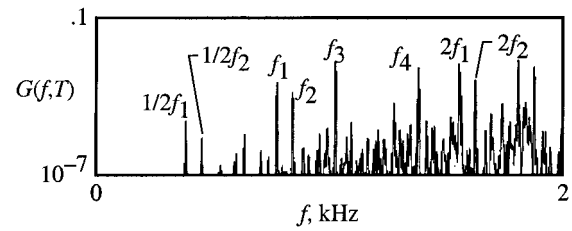

b) Panel *r* response

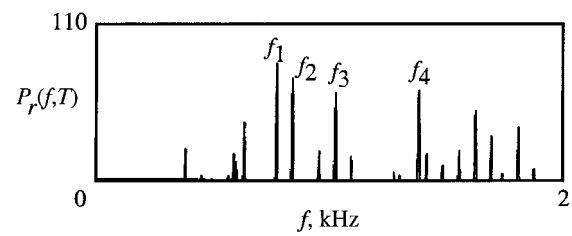

c) Transmitted pressure

Fig. 4 Spectral density of the initial forcing.

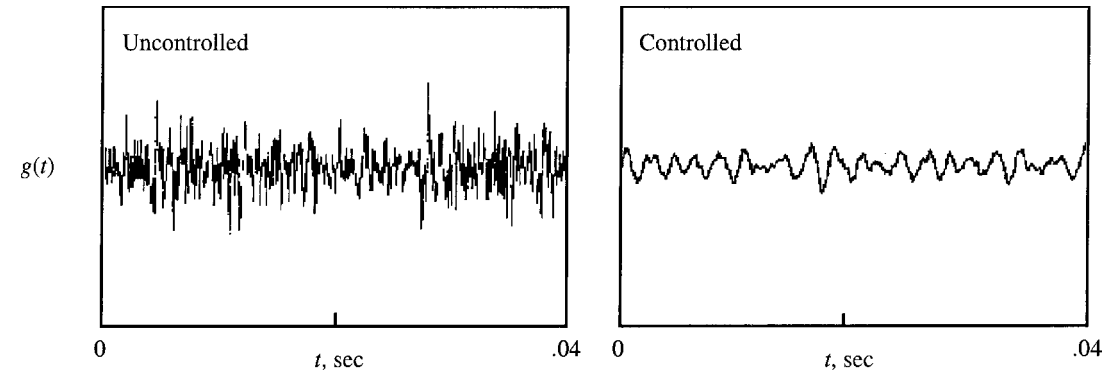

a) Measured acceleration response

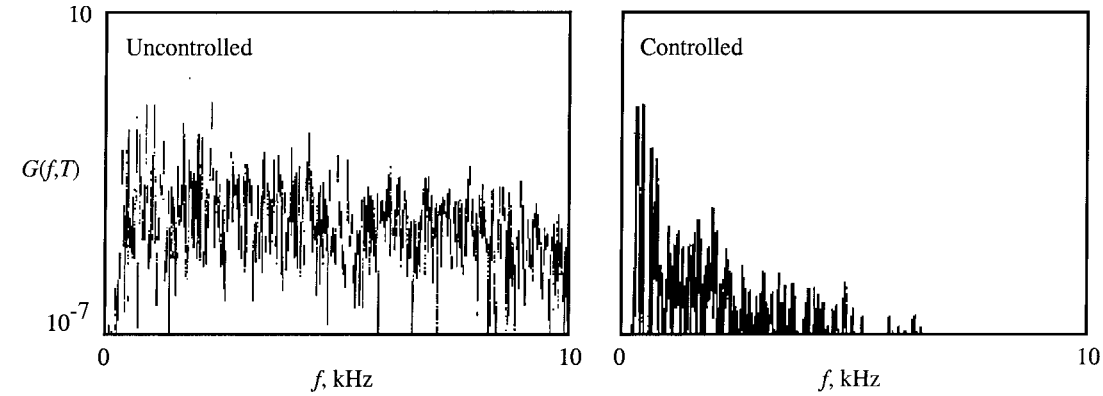

b) Computed power spectral density

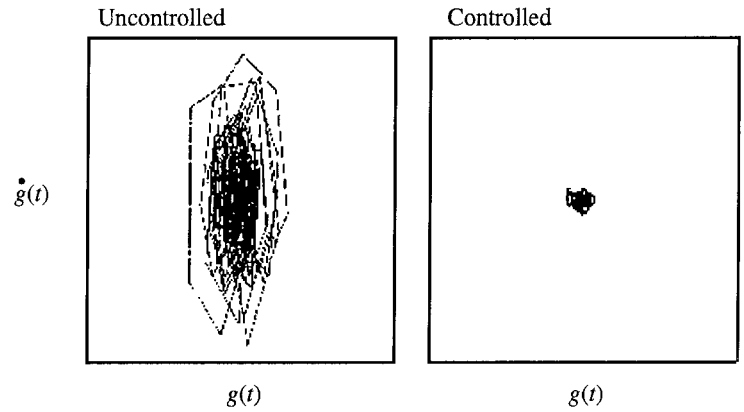

c) Computed phase plot

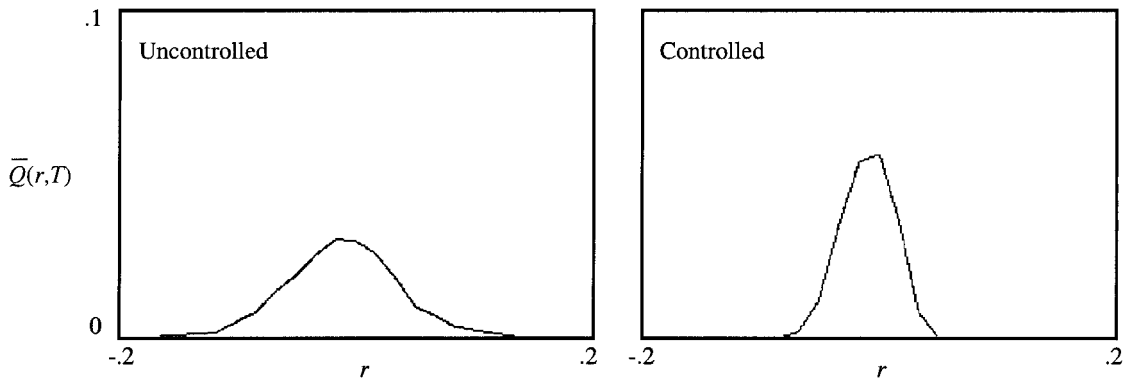

d) Computed probability density

Fig. 5 Panel acceleration response at one-quarter panel length.

is induced by the sound from four nonharmonic frequencies corresponding to $f_1 = 387$, $f_2 = 425$, $f_3 = 512$, and $f_4 = 687$ Hz. The measured real-time pressure $p(t)$ of the time series over the interval T, the computed power spectral density $P(f, T)$, the phase plots of the computed $\dot{p}(t)$ vs $p(t)$, and the computed probability density $Q(r, T)$ are shown in Fig. 2. The real-time wall pressure $p(t)$ shown for an interval of 0.079 s, T, is used to evaluate the spectrum, phase, and probability. The time series of the data is not periodic over a short or over an extended time, the spectrum is dominated by four basic forcing frequencies and harmonics, the phase plot indicates divergency and nonsymmetry in time, and the probability plot is not a normal distribution. Simultaneous pressure measurements at several locations along the tear stopper indicate minor variations in amplitude and phase. The analysis suggests that the wall pressure data came from few degrees of freedom, and it is natural to look to the low frequencies and large scale as the origin of the low-dimensional signals.

B. Panel Response

We analyze the case where the features of the nonlinear vibrations that arise are completely determined by the initial forcing conditions. Namely, the initial forcing conditions will play a role in the driving parameters that determine the response and the role for controlling it.

1. Search for Initial Forcing Parameters on Long-Term Response

Because the loading increases from the start, initial bifurcations are observed with the formulation of subharmonic and harmonic responses in a similar manner observed by Maestrello et al.[36] It is well known that the periodic forcing of a nonlinear dissipative dynamic system can lead to chaos. Similar to the sensitive dependence on the initial forcing, the chaotic transition depends sensitively on the initial forcing, such as the amplitude and frequency of the forcing. Because it has such a sensitive dependence on the initial forcing parameter, the idea of using a weak periodic external force to control the chaos has been suggested.

In the experimental investigation, the dynamic system is governed by the nonlinear partial differential equation for a curved elastic panel. The system might be expected to behave in an analogous manner to the periodically forced Duffing–Holmes equation, and the control strategy is based on this idea (see Ref. 37). Control technique was illustrated in the papers by Braiman and Goldhirsch[8] and Chacon and Bejarano[38] among others.

The forcing function is assumed to be quasi periodic of the form

$$p(a, \omega, t) = \sum_{i=1}^{n} a_i \cos(\omega_i t + \phi_i)$$

with given forcing parameters equal to the amplitudes $(a_1, a_2, \ldots, a_n) = a$, the circular frequencies $(\omega_1, \omega_2, \ldots, \omega_n) = \omega$, and the phases $\phi_1, \phi_2, \ldots, \phi_n$, where the frequencies are assumed to be incommensurate. Theoretically the transition to chaos caused by quasi-periodic forcing is not well understood. Based on the result of the monofrequency forcing, it is possible to suppose that the chaotic transition due to a quasi-periodic forcing depends on the initial forcing parameters a_i and ω_i as well. The experimental result seems to confirm this conjecture.

In the experimental study, for the initial forcing field, the wall pressure p is induced by an acoustic incident plane wave with four given frequencies: $f_1 = 387$, $f_2 = 425$, $f_3 = 512$, and $f_4 = 687$ Hz, where $f_i = \omega_i / 2\pi$, $i = 1, 2, 3, 4$.

To begin, the initial forcing amplitudes a_i are kept small. As time progresses, the amplitude is increased gradually to drive the system into a chaotic state. In each run, the panel response $g(t)$ (the panel acceleration) and transmitted acoustic pressure $p_r(t)$ are measured. The results show that the chaotic panel response depends strongly on the forcing conditions, the parameters a_i in this case. The acceleration response $g(t) = \mathrm{d}^2 w / \mathrm{d}t^2$ of the panel, as the amplitudes a_i increase in time to a set of constant postchaotic transition values, is shown in Fig. 3, where a nonsymmetrical panel response $g(t)$ is indicated in the chaotic regime. Based on the measured data, the finite time T, the wall pressure $p(t)$, the panel response $g(t)$, and the transmitted pressure $p_r(t)$ and, then, by the Fourier transform, the corresponding spectral density functions of the wall pressure $P(f, T)$, the panel response $G(f, T)$, and the transmitted pressure $P_r(f, T)$ are calculated. At low frequency, a comparison of the spectral density is made in Fig. 4. As expected, the wall pressure spectrum $P(f, T)$ shows peaks at the four initial frequencies f_1–f_4. The panel response spectrum $G(f, T)$ exhibits robust peaks at the same four forcing frequencies, f_1–f_4 and, in addition, at the subharmonics $1/2 f_1$ and $1/2 f_2$ as well as the harmonics $2 f_1$ and $2 f_2$. The other peak frequencies are incommensurable. The transmitted pressure spectrum $P_r(f, T)$ also shows the same four forcing frequencies with subharmonics and harmonics. Thus, from the experimental evidence, it is seen that at low frequencies, the four basic forcing

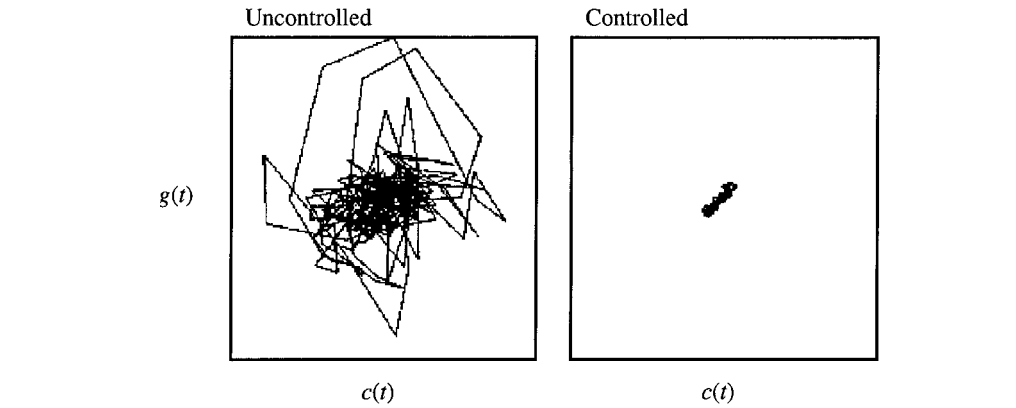

Fig. 5 Panel acceleration response at one-quarter panel length (continued).

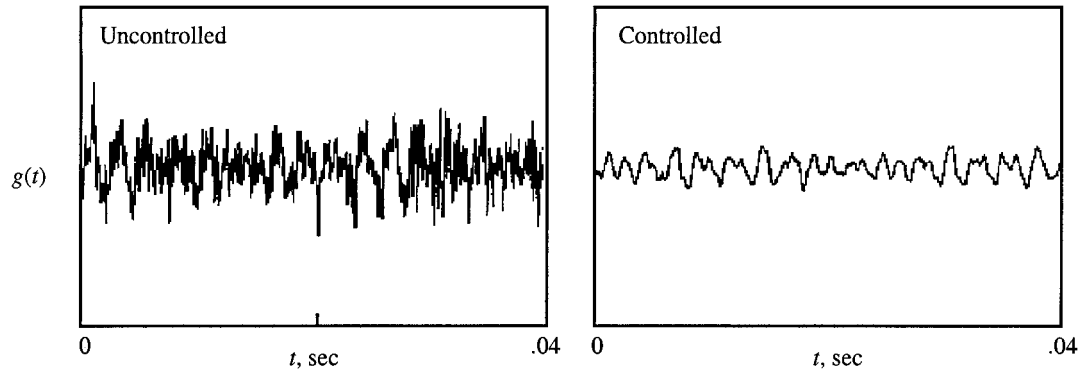

a) Measured acceleration response

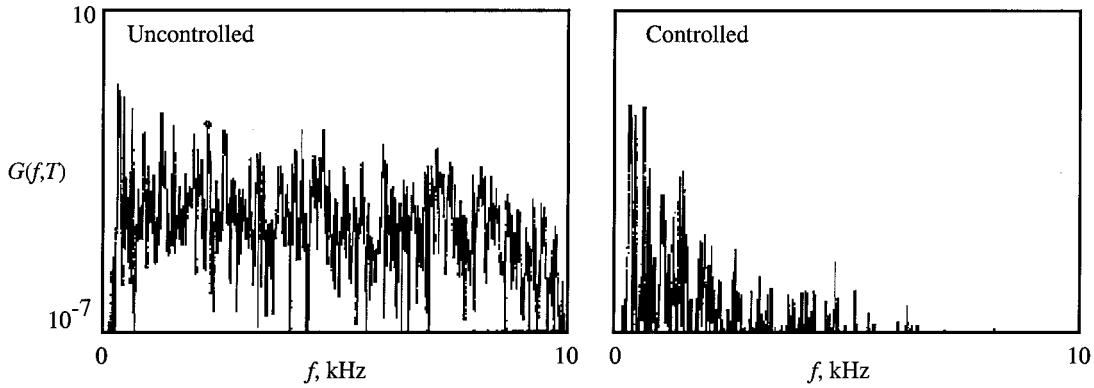

b) Computed power spectral density

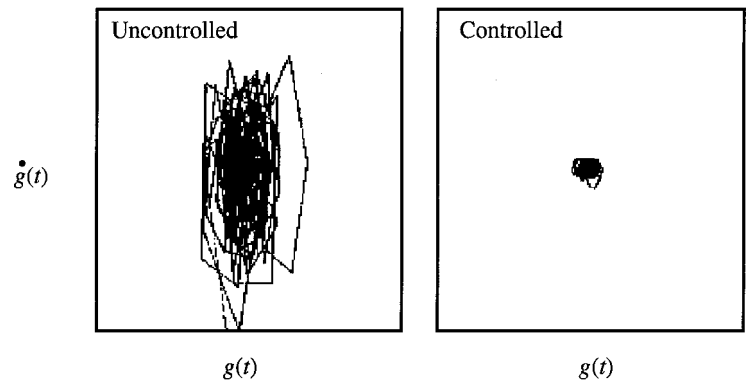

c) Computed phase plot

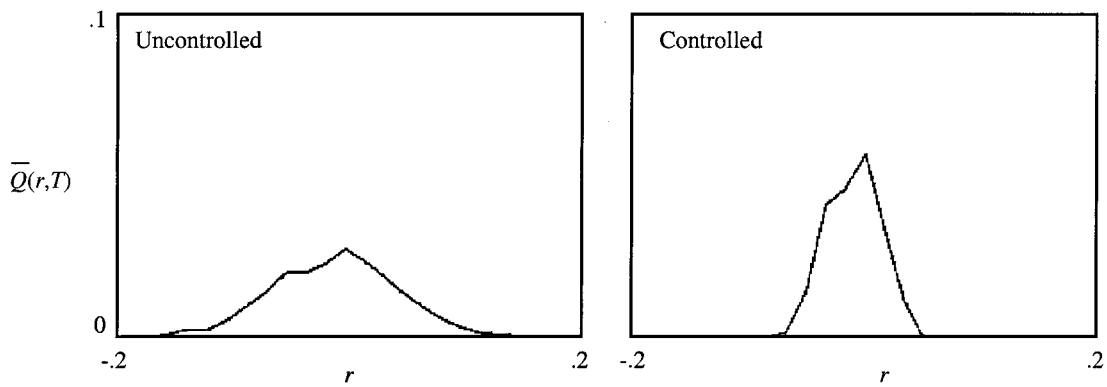

d) Computed probability density

Fig. 6 Panel acceleration response at three-quarter panel length.

frequencies f_1–f_4 appear prominently in both the panel response and the transmitted pressure power spectra.

To suppress the chaos, in view of the sensitive dependence on the initial forcing parameters, it is sensible to use a weak forcing $u(\varepsilon, \omega, \theta, t)$ as a control. Previous experiments indicate that nonlinearity and chaos are sensitive to the initial loading conditions.[36] In particular, u is taken to be

$$u(\varepsilon, \omega, \theta, t) = \sum_{i=1}^{4} \varepsilon_i \cos(\omega_i t + \theta_i)$$

where ω_i, $i = 1, 2, 3, 4$, represents the initial forcing frequencies and the amplitudes ε_1, ε_2, ε_3, and ε_4, which are small, and the phases θ_1, θ_2, θ_3, and θ_4 are to be adjusted experimentally to suppress the chaos. In practice the forcing frequencies f_i need not be known. Then, at least for the low-frequency case, they may be identifiable, amid the subharmonics and harmonics, from the peak frequencies in the panel response and transmitted pressure power spectra $G(f, T)$ and $P_r(f, T)$. Such peak frequencies are selected as possible forcing frequencies as a trial control function u. The possibility is tested in Secs. IV.B.2 and 3 as part of the chaos control strategy.

2. Uncontrolled and Controlled Response from Multifrequency Loading

Measurements of the panel response are made simultaneously at two points along the centerline, at one-quarter and three-quarter length. Figures 5 and 6 show the acceleration response $g(t)$ of the time series over the time interval T, the computed power spectral density $G(f, T)$, phase plot of the computed $\dot{g}(t)$ vs $g(t)$, and the computed probability density $\bar{Q}(r, T)$. Also, panel response $g(t)$ vs controller response $c(t)$ are shown in Fig. 5. A particular feature of the power spectra is the appearance of numerous incommensurate frequencies mixed with harmonics and subharmonics. The abrupt changes occurring in the time series have been previously observed[39] to be the result of frequency locking among previously incommensurate frequencies. Then the appearance of chaos, behind the locking state, was described to be the loss of synchronization between frequency locked modes. The temporal evolution of the power spectra showed pulsating chaotic behaviors from nonlinear coupling among mode waves. We determine whether the nonlinear determinism can be detected even when mixed with probable noise from the measured time series. We estimate the dimension and Lyapunov exponent over a finite time interval T. The results indicate that some exponents are positive (see Sec. V). The response of the two accelerometers symmetrically placed on the panel indicates loss of correlation for high input level and indicates correlation at lower input level. The difference in response between accelerometers is shown by the time series in Figs. 5a and 6a, and by the power spectra levels and distributions in Figs. 5b and 6b. The phase portrait plots are skewed indicating unsymmetrical response, and the probability plots are not a normal distribution and have a larger standard deviation than at a lower level in Figs. 5c, 5d, 6c, and 6d. The controller is virtually driven by the panel response in an uncontrolled state in Figs. 5e and 5f. In general, power spectra are very good for the visualization of periodic and quasi-periodic phenomena and their separation from chaotic time evolution. However, the analysis of chaotic responses themselves do not benefit much from the power spectra because they lose phase information, which is essential for the understanding of what happens on the strange attractor. In the latter case, the dimension of the attractor is no longer related to the number of independent frequencies in the power spectrum, and the dimension has been related to the concept developed for the experimental technique and data analysis in Sec. III, with details obtainable elsewhere.[34,35]

Active control of the panel response is achieved at low input power by using time-continuous control, carefully tuned at each initial forcing frequency. Active control is sensitively dependent on the initial forcing[40]; knowledge of it is a requirement for achieving control. There is no intelligent feedback between the system and actuation (Fig. 7). The broadband response is generated by four frequencies: $f_1 = 387$, $f_2 = 425$, $f_3 = 512$, and $f_4 = 687$ Hz (Figs. 5b and 6b). The controller is symmetrically placed between two accelerometers and driven at all initial forcing. The amplitude increases at each

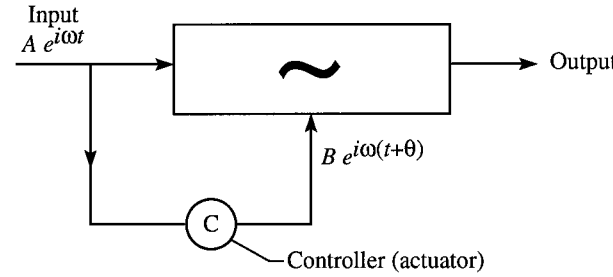

Fig. 7 Feedforward, open-loop control system.

forcing frequency when control is applied; the phases are adjusted to achieve control. Amplitude reduction starts at the highest frequencies. The amount is related to the power input to the controller for each forcing frequency selected during the initial part of the run. As the amplitude of the control frequencies increases, reciprocally the amplitude of all other frequencies decreases with slope greater than $1/f$. Results indicate that part of the energy is transferred from high to lower frequencies, while a very small part is dissipated. A simpler control mechanism was used in an earlier experiment in which the energy from the high-frequency harmonics, superimposed on a turbulent boundary layer in accelerated flow, accumulate into the fundamental through phase and amplitude tuning during the control process with very low dissipation.[10] In our present experiment, control is achieved by actively controlling all four frequencies (Sec. IV.B.1) through phase and amplitude tuning procedures with several stage adjustments. In stages, the controller forces the panel with amplitude and phase variations so that the energy of the high-frequency band is shifted toward the control frequency. Active control is not straightforward, and the desired control is not always achievable. The final results indicate that the medium- and high-frequency broadband response is reduced on the average by about 3 decades in amplitude. The time trace amplitude is also reduced, and the response changes into a quasi-periodic state.

3. Uncontrolled and Controlled Response from Monofrequency Loading

To widen the scope of the experiments, monofrequency loading $f = 1050$ Hz was used to illustrate the response and active control. Figures 8a and 8b show the uncontrolled and controlled power spectral density, an example in which the controller input is obtained with knowledge of the initial forcing of the panel dynamics. Results indicate that monofrequency loading can induce broadband response. Monofrequency loading and control have been reported on three unrelated experiments with the view of examining the energy transferred between mode waves to illustrate the role of initial forcing on control strategy using time series of the measured data.[40] Active control reduces the broadband spectrum to a periodic spectrum, fundamental and harmonics. The harmonic frequencies have similar amplitudes, whereas the control spectrum for multifrequency excitation (Figs. 5b and 6b) showed rapid decay.

Figure 8c shows an additional example of controlled power spectral density, in which the controller frequency $f = 2100$ Hz does not correspond to the forcing frequency $f = 1050$ Hz. This is a case in which control is applied indiscretely at some (arbitrary) peak frequency. This example demonstrates that when the control frequency does not correspond to the forcing frequency, control is not achievable via the stability approach. Figure 8c indicates that spectrum level and distribution are virtually unaffected when compared with Fig. 8a. From the experiment, we learn that, when the control frequency does not correspond to the initial forcing, control can be achievable by destructive interference, which requires that the controlling power approach the loading power. On the other hand, when control is obtained with the use of the initial forcing, the power required is very small.

V. Correlation Dimension and Lyapunov Exponents

The possibility of derived relationships between the correlation dimension D and Lyapunov exponents by using the Grassberger and Procaccia algorithm has been previously described.[32] The fundamental role played by Lyapunov exponents in defining chaotic

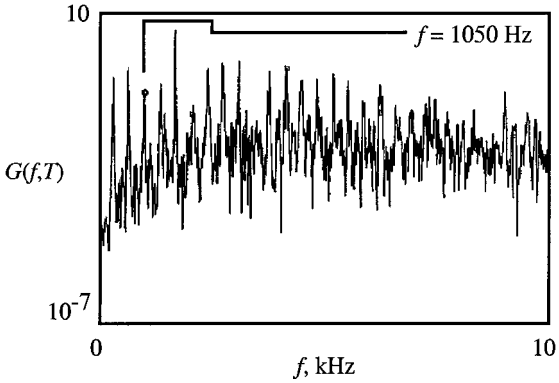

a) Uncontrolled with initial condition

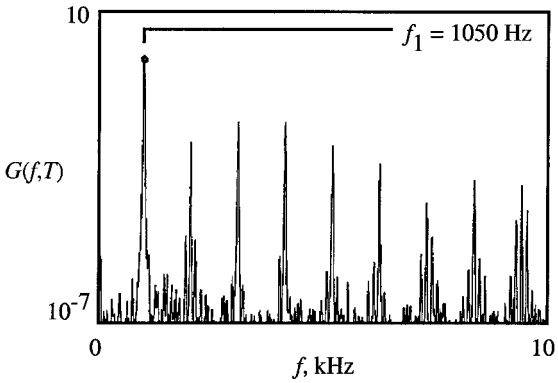

b) Controlled with initial condition

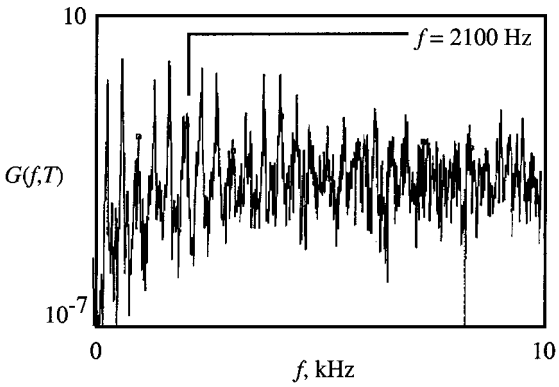

c) Controlled with different initial condition

Fig. 8 Panel accelertaion response at one-quarter panel length single frequency loading.

dynamics has stimulated the search for a statistical framework within which the accuracy of estimated exponents might be quantified.[30] Confidence bounds on estimation are of great interest. Experimental observations are limited, and it is in the finite time that Lyapunov exponents are of interest in our data analysis. The dimension of the attractor was determined to be related to the number of degrees of freedom of the panel response, a method described by Abraham et al.,[11] Ruelle,[30] Screenivasan,[41] and Sahay and Screenivasan.[42] To compute the dimension, we choose a range of size over which the scaling is to be estimated. The number of dimensions of the panel response increases with the increase in acoustic power level. The computation procedures have been previously illustrated by Maestrello[16] and Conte and Dubois.[33]

Figure 9 shows the computed exponents λ_2, λ_4, and λ_6 vs the embedding time $(D-1)\tau$ obtained from the acceleration response of the panel from the time data typical of the uncontrolled response shown in Fig. 5a. Only the values of the positive exponents are shown; most of the exponents are negative. Even a single positive exponent is sufficient proof that the attractor of the system is chaotic. As a conservative rule, 16 bit of precision are used for the experimental calculations. When the panel input acoustic loading is

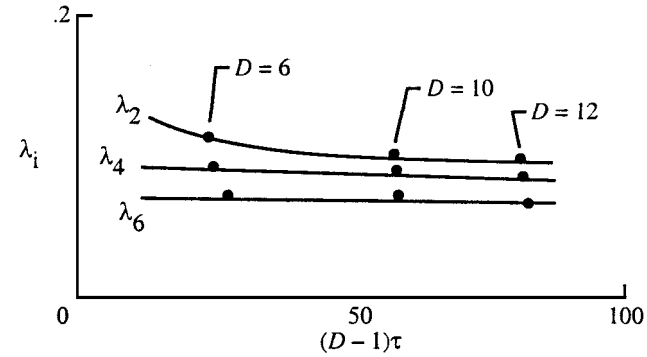

Fig. 9 Lyapunov exponent function of embedding time.

reduced, the largest Lyapunov exponent values decrease, and they become negative.

VI. Conclusions

Two selected examples of active control of broadband chaos response on a panel structure have been illustrated. Many others could be cited. Much effort has been spent on the control of chaos because in practice it may be impossible to avoid. We have observed the inherent sensitivity of the elastic panel response to initial forcing. Chaos response was anticipated from the experimental time series and by the numbers of subharmonics and harmonics in the spectra. The chaotic state has low-dimensional influence views from the Lyapunov exponent test. The loading is temporally chaotic and weakly spatiotemporally correlated.

We experimented with the controlling mechanism using small perturbations about the initial forcing with controlling signal power far below the power produced by the chaotic system response. The complexity of chaos and the sensitivity to small perturbations to initial condition are combined to control the responses. We demonstrated stabilization and control of chaos on time-continuous feedback, carefully tuned to each initial forcing. Control is easy to implement; it stabilizes broadband chaos on a panel efficiently and is resistive to exterior noise.

Destructive interference and damping are the two most popular control methods in the literature; however, they are not part of the rapid progress made in understanding the dynamics of deterministic nonlinear systems, especially chaos, initial forcing, and control by low-power feedback.

Finally, some practical guidelines indicate that active control is achievable because the initial forcing is determined. In a flight experiment where the structural response is related to the load, that is, the wall pressure difference, the initial forcing needs to be determined so that the stability control law may be efficiently applied. These developments have raised further new interesting questions and potentialities.

References

[1] Ott, C., Grebogi, E., and Yorke, J. A., "Controlling Chaos," *Physical Review Letters*, Vol. 64, No. 11, 1990, pp. 1196–1199.

[2] Epureanu, B. I., and Dowell, E. H., "System Identification for the Ott–Grebogi–Yorke Controller Design," *Physical Review E*, Vol. 56, No. 5, 1997, pp. 5327–5331.

[3] Ditto, W. L., Rauseo, S. N., and Spano, M. L., "Experimental Control of Chaos," *Physical Review Letters*, Vol. 65, No. 26, 1990, pp. 3211–3214.

[4] Hunt, E. R., "Stabilizing High-Periodic Orbits in a Chaotic System; The Diode Resonator," *Physics Letters*, Vol. 67, 1991, p. 1953.

[5] Petrov, V., Peng, B. O., and Showalter, K., "A Map-Based Algorithm for Controlling Low Dimensional Chaos," *Journal of Chemical Physics*, Vol. 96, No. 10, 1992, pp. 7506–7513.

[6] Garfinkel, A., Spano, M. L., Ditto, W. L., and Weiss, J., "Controlling Cardiac Chaos," *Science*, Vol. 257, Aug. 1992, pp. 1230–1235.

[7] Chow, P. L., and Maestrello, L., "Vibration Control of a Nonlinear Elastic Panel," Inst. for Computer Applications in Science and Engineering, ICASE Rept. 98-46, NASA CR-1998-208734, 1998.

[8] Braiman, Y., and Goldhirsch, I., "Taming Chaotic Dynamics With Weak Periodic Perturbations," *Physical Review Letters*, Vol. 66, No. 20, 1991, pp. 2545–2548.

[9]Corron, N. J., Pathel, S. D., and Hopper, B. A., "Controlling Chaos With Simple Limits," *Physical Review Letters*, Vol. 86, No. 17, 2000, pp. 3835–3838.

[10]Maestrello, L., "Active Control of Panel Oscillation Induced by Accelerating Boundary Layer and Sound," *AIAA Journal*, Vol. 35, No. 5, 1997, pp. 796–801.

[11]Abraham, N. B., Gollub, J. P., and Swinney, H. L., "Testing Nonlinear Dynamics," *Physica*, Vol. 11D, No. 1–2, 1984, pp. 252–264.

[12]Dowell, F. H., and Pezeshki, C., "On the Understanding of Chaos in Duffin Equations, Including a Comparison With Experiment," *Journal of Applied Mechanics*, Vol. 53, No. 1, 1986, pp. 5–9.

[13]Casdagli, M. C., Iasemidis, L. D., Sackellares, J. C., Roper, S. N., Glimore, E. L., and Savit, R. S., "Characterizing Nonlinearity in Invasive EEG Recording from Temporal Lobe Epilepsy," *Physica*, Vol. D99, No. 2–3, 1996, pp. 381–399.

[14]Sugihara, G., and May, R. M., "Nonlinear Forecasting as a Way of Distinguishing Chaos From Measurement Error in Time Series," *Nature*, Vol. 344, April 1990, pp. 734–754.

[15]Abarbanel, D. I., Brown, R., and Kadtke, J. B., "Prediction of Chaotic Nonlinear System: Methods for Time Series With Broadband Fourier Spectra," *Physical Review A: General Physics*, Vol. 41, No. 4, 1990, pp. 1782–1807.

[16]Maestrello, L., "Chaotic Response of Panel Vibrations Forced by Turbulent Boundary Layer and Sound," *AIAA Journal*, Vol. 37, No. 3, 1999, pp. 289–295.

[17]Nayfeh, A. H., and Mook, D. T., *Nonlinear Oscillation*, Wiley, New York, 1979, pp. 62–97.

[18]Virgin, L. N., and Dowell, E. H., "Nonlinear Aeroelasticity and Chaos," *Computational Nonlinear Mechanics in Aerospace Engineering*, edited by S. N. Aturi, AIAA, Washington, DC, 1992, pp. 531–541.

[19]Dowell, E. H., "Chaotic Oscillations in Mechanical Systems," *Computational Mechanics*, Vol. 3, 1988, pp. 199–216.

[20]Mei, C., "A Finite Element Approach for Nonlinear Panel Flutter," *AIAA Journal*, Vol. 15, No. 8, 1997, pp. 1107–1110.

[21]Mei, C., Adebel-Motagaly, K., and Chen, R., "Review of Nonlinear Panel Flutter at Supersonic and Hypersonic Speeds," *Proceedings of the CEAS/AIAA/ICASE/NASA LRC International Forum on Aeroelasticity and Structural Dynamics*, Vol. 2, 1999, pp. 479–497.

[22]Bolottin, V. V., Grishko, A. A., Kounadis, A. N., Gantes, C., and Robert, J. B., "Influence of Initial Conditions on the Postcritical Behavior of a Nonlinear Aeroelastic System," *Nonlinear Dynamics*, Vol. 15, 1998, pp. 63–81.

[23]Abarbanel, H. D. I., Brown, R., Sidorowich, J. J., and Tsimring, L. S., "The Analysis of Observed Chaotic Data in Physical Systems," *Reviews of Modern Physics*, Vol. 65, No. 4, 1993, p. 1331.

[24]Geist, K., Parlitz, U., and Lauterborn, W., "Comparison of Different Methods for Computing Lyapunov Exponents," *Progress of Theoretical Physics*, Vol. 83, No. 5, 1990, pp. 875–893.

[25]Fenno, C. C., Bayliss, A., and Maestrello, L., "Interaction of Sound From Supersonic Jets with Nearby Structures," *AIAA Journal*, Vol. 36, No. 12, 1998, pp. 2153–2162.

[26]Glass, L., and Mackey, M., "Pathological Conditions Resulting from Instabilities in Physiological Control System," *Annual of the New York Academy of Science*, Vol. 316, 1979, p. 214.

[27]Fuller, C. R., *Active Control of Vibration*, Academic Press, London, 1996.

[28]Aguirre, L., and Billings, S. A., "Validating Identified Nonlinear Models With Chaotic Dynamics," *Intl. J. Bifur. Chaos in Appl. Sci. Eng.*, Vol. 4, No. 1, 1994, pp. 109–126.

[29]Theiler, J., Eubank, S., and Farmar, J. D., "Testing for Nonlinearity in Time Series: The Method of Surrogate Data," *Physica D*, Vol. 58, No. 1–4, 1992, pp. 77–94.

[30]Ruelle, D., "The Claude Bernard Lecture, 1989, Deterministic Chaos: The Science and Fiction," *Proceedings of the Royal Society of London, Series A: Mathematical and Physical Sciences*, Vol. A472, Feb. 1990, pp. 241–248.

[31]Abarbanel, H. D. I., *Analysis of Observed Chaotic Data*, Springer-Verlag, Berlin, 1996, pp. 25–112.

[32]Grassberger, P., and Procaccia, I., "Measuring the Strangeness of Strange Attractors," *Physica D*, Vol. 9, No. 1–2, 1983, pp. 189–208.

[33]Conte, R., and Dubois, M., "Lyapunov Exponents of Experimental System," Nonlinear Evolutions, edited by J. P. D. Leon, World Scientific, Singapore, 1988, pp. 767–780.

[34]Eckmann, J. P., and Ruelle, P., "Ergotic Theory Strange Attractor," *Review of Modern Physics*, Vol. 57, No. 3, Pt. 1, 1985, pp. 616–656.

[35]Eckmann, J. P., Kamphorst, O., Ruelle, D., and Ciliberto, S., "Lyapunov Exponents for Time Series," *Physical Review A: General Physics*, Vol. 34, No. 6, 1986, pp. 4971–4979.

[36]Maestrello, L., Frendi, A., and Brown, D. E., "Nonlinear Vibration and Radiation from a Panel with Transition to Chaos," *AIAA Journal*, Vol. 30, No. 11, 1992, pp. 2632–2638.

[37]Guckenheimer, J., and Holmes, P., *Nonlinear Oscillation in Dynamical Systems and Bifurcation of Vector Fields*, Springer-Verlag, New York, 1983, pp. 82–91.

[38]Chacon, R., and Bejarano, J. D., "Routes to Suppressing Chaos by Weak Periodic Perturbations," *Physical Review Letters*, Vol. 71, No. 19, 1993, pp. 3103–3106.

[39]Gao, J. Y., Narducci, L. S., Schulman, M., Squicciarini, M., and Yuan, J. M., "Route to Chaos in a Hybrid Bistable System With Delay," *Physical Review*, Vol. A28, No. 5, 1983, p. 2910.

[40]Maestrello, L., "Active Control by Conservation of Energy Concept," *AIAA Journal* (submitted for publication); also AIAA Paper 2000-2045, June 2000.

[41]Sreenivasan, K. R., "Transition of Turbulent in Fluid Flow and Low Dimensional Chaos," *Frontier in Fluid Mechanics*, edited by S. H. Davis and J. M. Lumley, Springer-Verlag, Berlin, 1985, pp. 41–67.

[42]Sahay, A., and Sreenivasan, K. R., "The Search for a Low-Dimensional Characterization of a Local Climate System," *Philosophical Transactions of the Royal Society of London, Series A: Mathematical and Physical Sciences*, Vol. A354, No. 1713, 1996, pp. 1715–1750.

P. J. Morris
Associate Editor